coatings

MDPI

Article

Effect of TiO_2@$CaCO_3$ Waterborne Primer on the Coloring Performance of Inkjet-Printed Wood Product Coatings

Ruijuan Sang [1,2,*] and Fei Yang [1,2]

[1] College of Furnishings and Industrial Design, Nanjing Forestry University, Nanjing 210037, China; yangfei@njfu.edu.cn
[2] Co-Innovation Center of Efficient Processing and Utilization of Forest Resources, Nanjing Forestry University, Nanjing 210037, China
* Correspondence: sangruijuan@njfu.edu.cn

Abstract: Calcium carbonate ($CaCO_3$) is a widely used inorganic filling pigment used in coatings, and it is known for its nontoxicity, odorlessness, and environmental friendliness. The application of $CaCO_3$ as a filler can effectively reduce raw material costs, and optimization of the filler formula enhances the coating film performance. In this study, oak planks were prepared as substrates for water-based inkjet printing. Three composite water-based primers with different TiO_2-to-$CaCO_3$ ratios and a polyurethane resin primer were used to prepare the substrate for the printing surface. The properties of the water-based primer coating and the water-based inkjet printing coating were characterized and analyzed via Fourier-transform infrared spectroscopy, video-based contact angle analysis, and environmental scanning electron microscopy. The aim was to investigate the effects of the composite waterborne primer coatings on the ink absorption and coloring properties of the interface between wood substrates and waterborne inkjet coatings. Sample WDCC-3#, with a TiO_2-to-$CaCO_3$ ratio of 15:35, exhibited the most comprehensive characteristics. The wood surface coated with 15 g/m^2 of the polyurethane resin primer and 15 g/m^2 of WDCC-3# exhibited a 5.8° contact angle of the water-based ink, first-grade adhesion, 4 H hardness, 70.52 whiteness value, and a roughness of ~2.33. The surface of the printed water-based inkjet-coated substrate was uniform and smooth, featuring rounded and transparent edges of the water-based ink droplets and a small CMYK color difference value. Therefore, the composite waterborne primer, incorporating TiO_2 and $CaCO_3$ in specific ratios, can be effectively combined with waterborne polyurethane primer coatings. This combination significantly improves the interfacial compatibility between the oak surface and waterborne inkjet coatings, leading to enhanced ink absorption on the oak plank surface during printing. This results in a high degree of color reproduction and clearer printed images. Overall, this study provides valuable insights for the development of primer programs for the industrial application of waterborne digital inkjet technology on wood products.

Keywords: waterborne primer; calcium carbonate; water-based ink; oak plank; inkjet printing technology

check for updates

Citation: Sang, R.; Yang, F. Effect of TiO_2@$CaCO_3$ Waterborne Primer on the Coloring Performance of Inkjet-Printed Wood Product Coatings. *Coatings* **2023**, *13*, 2071. https://doi.org/10.3390/coatings13122071

Academic Editor: Marko Petric

Received: 8 November 2023
Revised: 7 December 2023
Accepted: 8 December 2023
Published: 12 December 2023

Copyright: © 2023 by the authors. Licensee MDPI, Basel, Switzerland. This article is an open access article distributed under the terms and conditions of the Creative Commons Attribution (CC BY) license (https://creativecommons.org/licenses/by/4.0/).

1. Introduction

In recent years, the environmentally friendly and healthy properties of water-based printing ink [1,2] have gradually attracted increasing attention. Moreover, the market share of water-based printing ink has grown significantly, especially within the wood product printing industry. Water-based inkjet printing on wood surfaces does not require plate making and allows for the flexible setting of the printing quantity, style, and effect [3]. Moreover, water-based ink uses water, rather than organic solvents, as a solvent or dispersion medium. This saves a large amount of organic material resources, reduces environmental pollution caused by the volatilization of organic solvents in coatings, mitigates physical hazards to construction personnel, and minimizes fire hazards during construction [4]. However, the use of water-based ink in wooden products is characterized by low raw

material utilization, high energy consumption, and low product-added value due to production requirements [5,6], mainly because of the difficulty of directly using wood with surface defects such as scabs, scratches, and cracks [7]. Furthermore, lignin in wood contains many colored components, and the water-based ink-coating film turns yellow after drying, resulting in an excessive color deviation from expected values [8]. Therefore, a primer-application process to promote interfacial fusion between coatings is required. A primer is an essential coating for connecting the surface coating and the substrate in the entire supporting system of the wood coating design [9,10].

In previous studies, primer polymer films have been used in wood-related applications [11–13]. For example, a study on flame-retardant wood revealed that only the synergistic effect between the primer and the plasma layer could lead to flame retardancy, and the primer helped to smooth the surface of the plasma coating, seal the pores of the wood, and promote the formation of a more uniform plasma layer [11]. In wood 3D printing, primer can achieve a high bonding strength [14]. The mechanical properties of UV-cured multilayer wood coating systems can be improved by optimizing the composition and thickness of the primer [15,16]. In addition, the UV inkjet technology [17] requires a white background substrate to match the conventional colors, and there is an adhesion issue with conventional top coating used as a base for direct inkjet printing [18]. Therefore, the primer-treated substrate can improve the mechanical properties and printing quality of the paint film [19]. However, research on water-based primer [20,21] printing systems for wood applications is still limited, and research on the coloring performance of wood product coatings needs to be addressed. To achieve good coloring performance between the wooden substrate and the upper water-based inkjet printing coating, the primer must have good concealing ability and high whiteness. TiO_2 and $CaCO_3$ are common fillers in paint production. TiO_2 is widely used in the paint industry due to its excellent pigment properties, such as a high refractive index, excellent hiding power, nontoxicity, high whiteness, and stability [22–24]. $CaCO_3$ is characterized by low cost, abundant reserves, high stability, and permeability, making it suitable for industrial use that requires mass production [22–25]. In addition, field research found that oak planks [19] are commonly used in the floor production line of solid wood materials. Their texture is firm, and they have beautiful grain, but part of the surface of the oak boards has scars, scratches, stains, and other defect phenomena. These defects do not damage the mechanical properties of the wood because of aesthetic problems and are difficult to utilize, while filler addition can cover defects, providing a stable substrate surface for water-based inkjet printing process steps.

This article mainly explores the effect of TiO_2@$CaCO_3$ composite water-based primer on the coloring performance of inkjet dyeing coatings. The purpose was to further refine the primer process for water-based inkjet printing on wood surfaces and to improve the ink absorption and coloring properties of oak substrates. The printing performances of three TiO_2@$CaCO_3$ primers with different TiO_2-to-$CaCO_3$ ratios on inkjet color ink layers are compared. The influence of the $CaCO_3$ filler content on the performance of water-based primers is investigated, which provides a basis for studying the excellent interface performance of water-based inkjet printing. Figure 1 shows the structure of water-based inkjet coating on the wood surface. This coating process is suitable for a wide range of porous substrates, but in practice, it needs to be adapted to the material's own characteristics to achieve better results. The bottom layer is an oak laminate, the intermediate layer is a primer roller-coated on the wood surface, and the top layer is the water-based inkjet printing layer and water-based topcoat abrasion-resistant sealing layer. This paper focuses on the intermediate primer layer to improve the compatibility between the water-based ink layer and the substrate and the colorability of the water-based inkjet pattern.

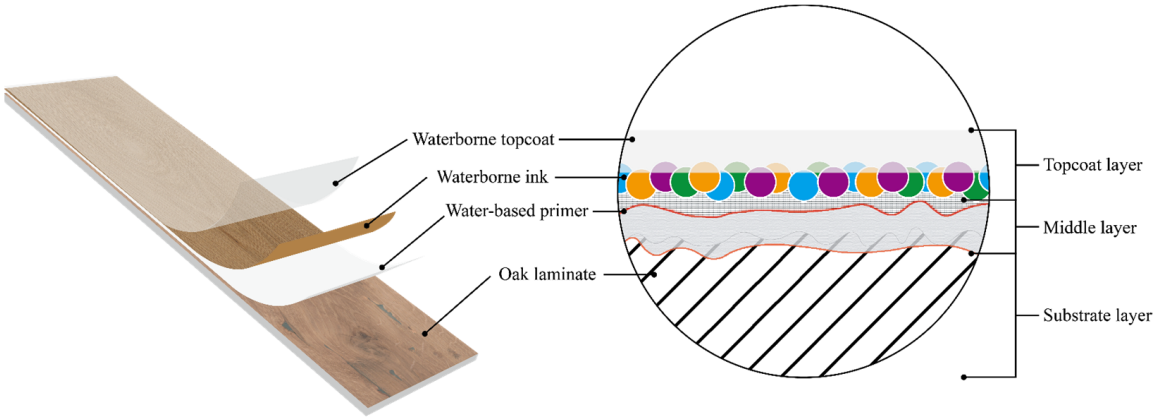


Figure 1. Schematic structure of water-based inkjet coating on wood surface.

2. Materials and Methods

2.1. Materials

For this experiment, calcium carbonate ($CaCO_3$) and titanium dioxide (TiO_2) were used as primer fillers, both procured from Shanghai Aladdin Biochemical Technology Co., Ltd. (Shanghai, China). Other raw materials for water-based primers and water-based polyurethane resin primers (model WD4500A) were provided by Jiangsu Haitian Technology Co., Ltd. (Jurong, China). The raw materials are detailed in Table 1. Additionally, CMYK water-based ink (cyan, magenta, yellow, and black, HONGSAM H5-D310) and an oak grain image (format: TIF, resolution: 300 dpi, size: 10 cm × 36 cm) were obtained from Nanjing Leili Digital Technology Co., Ltd. (Nanjing, China). Oak planks, known for their material color uniformity, served as substrates for inkjet printing coating (specification: 20 cm × 36 cm × 0.15 cm).

Table 1. Raw materials for the preparation of waterborne primer.

No.	Experimental Materials	Molecular Formula
1	H_2O	H_2O
2	pH regulator	-
3	Defoamer	-
4	Propylene glycol	$C_3H_8O_2$
5	Wetting agent	-
6	Dispersant	-
7	Titanium dioxide	TiO_2
8	Calcium carbonate	$CaCO_3$
9	Thickening agent	-
10	Acrylic lotion	$C_3H_4O_2$
11	Anti-settling agent	-
12	Film-forming aids	-
13	Foam inhibitor	-
14	Fungicide	-

Mark: (-) indicates that the molecular formula is not marked here.

2.2. Component Content of TiO_2@$CaCO_3$ Composite Waterborne White Primer

The modification of the component content in the waterborne primer was based on the improved exploration of waterborne polyurethane resin primers. The existing water-based polyurethane resin primers primarily serve as sealing and whitening agents, but their ink absorption ability is suboptimal, resulting in poor ink coloring ability. $CaCO_3$ and TiO_2 are necessary fillers in paint production, each with its advantages. The combination of the two fillers can endow water-based primer coatings with superior performance. Therefore, $CaCO_3$ and TiO_2 are mixed in this study to produce three water-based primers with different TiO_2-to-$CaCO_3$ ratios: WDCC-1$^{\#}$, WDCC-2$^{\#}$, and WDCC-3$^{\#}$ (Table 2).

Table 2. Composite primers with different TiO_2-to-$CaCO_3$ ratios.

No.	Raw Material	Proportion (Number of Copies)		
1	TiO_2:$CaCO_3$	WDCC-1# 5:45	WDCC-2# 10:40	WDCC-3# 15:35

2.3. Primer Preparation Process

Step 1: Water and the pH adjusting agent (RHODOLINE AN-130) were added to a container, and then the mixture was stirred at low speed. An antifoam agent, propylene glycol, wetting agent, and dispersant were slowly and sequentially added to the mixture, which was then dispersed at a low rate for 2 min. Step 2: Titanium dioxide and calcium carbonate were sequentially added to the mixture, and the mixture was stirred at low to medium speeds for 5 min. Step 3: A thickener was slowly added to the mixture, which was then stirred and subjected to high-speed dispersion for 10 min. A fineness of $\leq$30 µm was verified using an instrument (scraper bar fineness meter). Step 4: The mixture was mixed at low and medium speeds, an acrylic emulsion was added, and the mixture was mixed for an additional 5 min to enable dispersion. A medium speed was then adopted, an anti-settling agent was added, and the mixture was allowed to disperse for 5 min. Step 5: Film-forming additives, defoamer, and foam inhibitor were mixed in another container and dispersed at high speed for 10 min, and a shrinkage test was performed. Step 6: Water and fungicide were slowly added to the mixture, which was dispersed at medium speed. The mixture was then dispersed for an additional 2 min.

2.4. Method of Roller-Coating Water-Based Primer on Wood Surface

The primer roller-coating process adopted in this experiment is described as follows: The specific steps involving two coating processes are outlined in Table 3. First, all wood samples were coated with the same water-based polyurethane resin white primer. After the samples were subjected to infrared-light drying, each sample was roller-coated with each of WDCC-1#, WDCC-2#, and WDCC-3#, which gives energy doses of 200 J/cm^2. The water-based primer plates were then dried again with infrared light to obtain three water-based primer coating samples (Figure 2C).

Table 3. Process steps for the roller-coating of waterborne primer.

Step	Model	Product Name	Coating Amount/g/m^2	Function	Notes
1	WD4500A	Waterborne polyurethane resin white primer	15	Whitening and sealing	Double rubber roller/infrared drying
2	WDCC	TiO_2@$CaCO_3$ composite water-based white primer	15	Whitening and ink absorption	Double rubber roller/infrared drying

2.5. Testing and Characterization

2.5.1. Surface Tension Test

To assess the wettability of aqueous inks on oak plank substrates, a Theta t200 optical contact angle gauge (Biolin Technology Co., Ltd., Gothenburg, Sweden) was used. Three oak planks roller-coated with water-based primers with different TiO_2-to-$CaCO_3$ ratios were placed on a stage. The surface energy of the printing substrate was determined using the drop method. Specifically, five test points were randomly selected in the perpendicular direction of the tangential section, and about 1 µL of blue water-based ink was carefully dropped onto the substrate surface. The entire process, from the ink droplet making contact

with the sample surface to its diffusion during the microinjector sinking process, was observed, and the contact angle value was recorded.

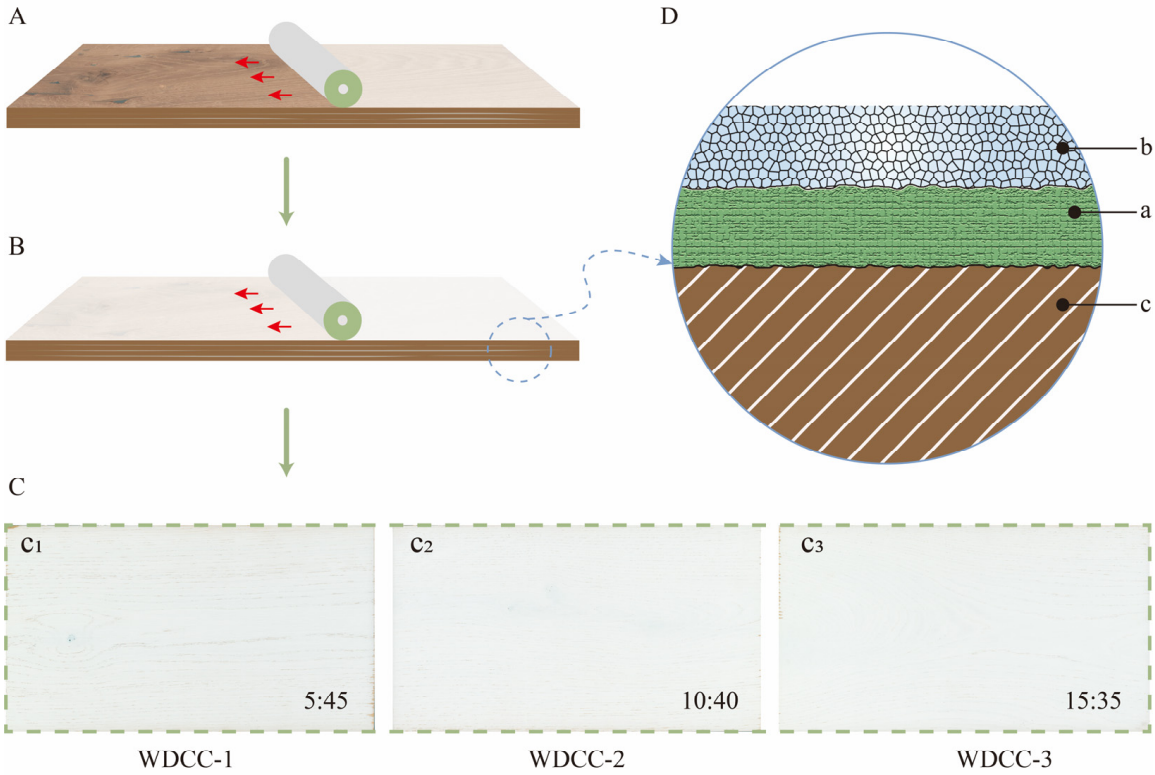


Figure 2. Process drawing of oak plank roller-coated with a primer. (**A**) First layer of coating with water-based polyurethane resin white primer; (**B**) Second layer of coating with a TiO_2@$CaCO_3$ composite water-based white primer; (**C**) Primer coatings with three TiO_2-to-$CaCO_3$ ratios ($\mathbf{c_1}$: WDCC-1, $\mathbf{c_2}$: WDCC-2, $\mathbf{c_3}$: WDCC-3); (**D**) Profile of water-based primer coatings (**a**: water-based polyurethane resin primer; **b**: TiO_2@$CaCO_3$ composite water-based white primer; **c**: Oak substrate).

2.5.2. Infrared Spectroscopy Testing

Surface functional group changes in the three samples were analyzed via infrared spectroscopy (VERTEX80V, Bruker Spectrometer, Germany). Samples were cut into blocks of approximately 5 mm × 5 mm × 2 mm and placed in the test chamber of an infrared spectrometer. The ATR (Attenuated Total Refraction) mode was employed to reflect the sample's surface and generate the sample's infrared spectrum. Subsequently, spectral peak changes on the surface of the three wood groups were compared and analyzed.

2.5.3. Surface Morphology Characteristics Obtained via Scanning Electron Microscopy

The micromorphologies of the three groups of water-based primer coatings were examined using a Quanta200 (FEI, Portland, OR, USA) environmental scanning electron microscope. This analysis involved the observation of element types and distribution areas within the water-based primer coating via energy-dispersive X-ray spectroscopy.

2.5.4. Optical Microscopy Observation

In a microscopic environment, the layout of ink dots in inkjet printing can be visually inspected. An optical microscope (CX23LEDRFS1C, Olympus Industrial Co., Ltd., Guangzhou, China) was used to observe the distribution of ink dots on the surface of the three sample sets.

2.5.5. Paint Film Performance Testing

Four CMYK color blocks were generated as standard test charts for the experiment. After these test charts were printed using a water-based inkjet digital printing device (E1613, Wuhan Mansi Electronic Technology Co., Ltd., Wuhan, China), the LAB values of the color blocks were measured with a spectrophotometer. The average color difference was calculated using the CIEDE2000 color difference formula ISO11664-6:2022 [26]. For example, to determine the color difference between L_1^*, a_1^*, b_1^* and L_2^*, a_2^*, b_2^* in the CIELAB color space, the color differences between the two were expressed as shown in Equation (1). The detailed calculation process is presented in the annex.

$$\Delta E_{00}(L_1^*, a_1^*, b_1^*;\ L_2^*, a_2^*, b_2^*) = \Delta E_{00}^{12} = \Delta E_{00}. \tag{1}$$

The CIEDE 2000 color difference ΔE_{00} is calculated as

$$\Delta E_{00} = \sqrt{\left(\frac{\Delta L'}{K_L S_L}\right)^2 + \left(\frac{\Delta C'}{k_c S_c}\right)^2 + \left(\frac{\Delta H'}{k_H S_H}\right)^2 + R_T\left(\frac{\Delta c'}{k_c S_c}\right)\left(\frac{\Delta H'}{k_H S_H}\right)} \tag{2}$$

The adhesion cross-cutting test of coatings was conducted following GB/T4893.4-2013 "Method for Determination of Surface Adhesion of Furniture" [27]. This test is used to evaluate the adhesion of surface coatings on wooden products. The degree of surface coating detachment is assessed on a scale of 0–5. A score of 0 is assigned when the cutting edge is completely smooth, with no grid detachment, while a rating level of 5 indicates a high degree of detachment at the edge of the grid. The glossiness of the coating was measured using an HG268 gloss meter, following GB 4893.6-2013 "Method for Measuring the Physical and Chemical Properties of Furniture Surface Paint Films—Gloss" [28]. Each group of test pieces underwent five parallel tests. When the glossiness at a 60° incidence angle is lower than 10 GU, the 85° incidence angle provides better resolution, and therefore, the 85° incidence angle was selected for measurement. Coating hardness was determined according to GB/T 6739-2006 "Pencil Method for Determination of Film Hardness of Paints and Varnishes" [29]. The QHQ-type coating pencil scratch hardness tester was used, and three specimens were tested in parallel for each group. Coating roughness was assessed using a JB-C roughness tester, and the average of measurements taken at five points on each specimen was taken as the result. The whiteness of the coating, which can affect color deviation in printing [30,31], was measured on the sample's surface using a WSB-2 whiteness meter (Qiwei, Hangzhou, China). Measurements were taken at five areas for each sample, and the average value was calculated.

3. Results and Discussion

3.1. Wettability Analysis of TiO_2@$CaCO_3$ Waterborne Primer Wood Coatings

Figure 3 displays the contact angle measurements on the surface of the untreated oak plank and the three composite waterborne primer coatings with different TiO_2-to-$CaCO_3$ ratios. The initial ink contact angle of untreated wood is 56.17°, and after stabilization for 50 s, the contact angle is 37.28°. The slight variation in contact angle size is due to several factors, such as the size of the grain pores in the wood cell walls and sediment clogging, which influence wood permeability. With the addition of the primer coating, the ink penetration amplitude gradually increases. This occurs because the higher the surface energy of the coating relative to the surface tension of the ink, the higher the coating's wettability, resulting in a smaller observed contact angle [32]. The initial ink contact angle of the WDCC-1$^{\#}$ oak plank plate is 51.21°, and after stabilization for 50 s, the contact angle is 27.8°. The initial ink contact angle of the WDCC-2$^{\#}$ oak plank is 58.89°, and after stabilization for 50 s, the contact angle is 12.84°. The initial ink contact angle of the WDCC-3$^{\#}$ oak plank plate is 37.21°, and after stabilization for 50 s, the contact angle is 5.8°. These results reveal that the hydrophilicity of the TiO_2@$CaCO_3$ composite water-based primer coating increases with an increasing TiO_2-to-$CaCO_3$ ratio, indicating that the composite

coating has a low contact angle and high surface energy. Furthermore, as the ratio of TiO_2 to $CaCO_3$ increases, the coating's ink absorption performance improves. Among the primers, WDCC-3# exhibits the best ink absorption performance because $CaCO_3$ promotes sedimentation and permeability of the primer on the base layer's surface [33]. A smaller contact angle corresponds to higher wettability, making the surface more receptive to liquid, thus facilitating surface coating [24]. Additionally, $CaCO_3$ is white and composed of fine particles that can be uniformly dispersed in paints; thus, it serves as a structural component. $CaCO_3$ also functions as a key body pigment extensively utilized in the paint industry.

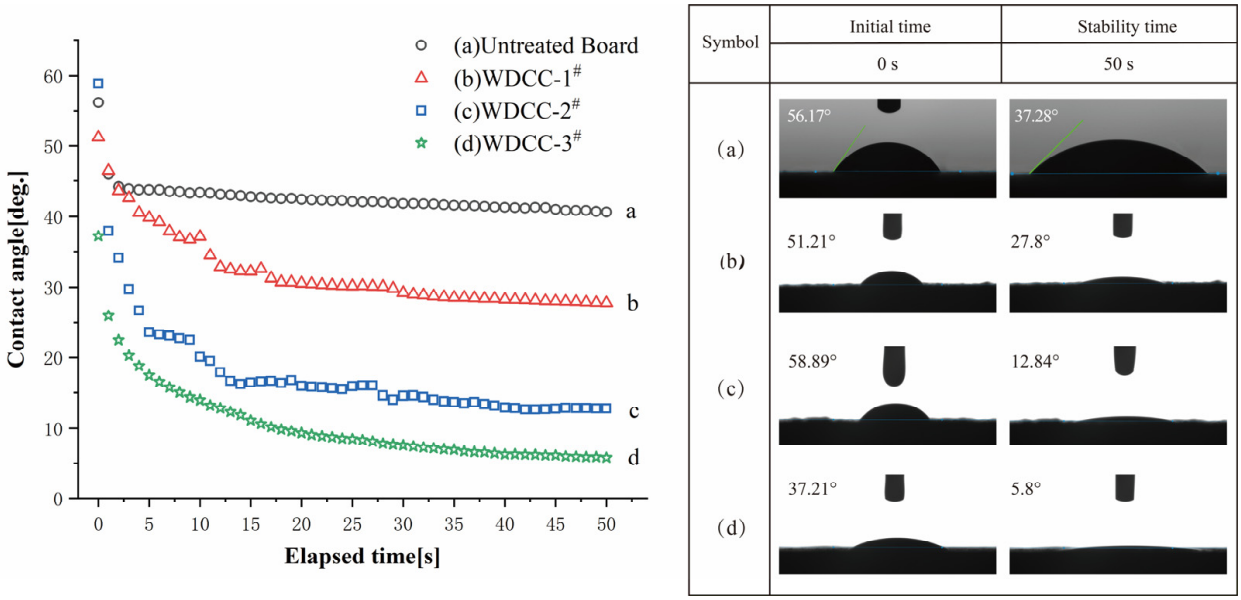


Figure 3. Contact angles of water-based primer coatings with different filler ratios.

3.2. Infrared Spectrometer Testing and Analysis

Infrared spectroscopy allows for the quantitative analysis of the chemical bonds and functional group structures of the three TiO_2@$CaCO_3$ composite water-based primers from a microscopic perspective. Figure 4a shows the untreated oak boards as a control. Figure 4b–d displays the infrared spectra of the three waterborne primer coatings with different TiO_2-to-$CaCO_3$ ratios. The peaks at 2920 cm^{-1} and 2849 cm^{-1} are attributed to vibration of -CH_3/-CH_2 groups [34]. The peak located at 1729 cm^{-1} is typical absorption of hydrogen bonded C=O groups [35]. The peaks at 1729, 1392, 872, and 708 cm^{-1} correspond to C=O stretching vibration, CH bending vibration, C–O out-of-plane deformation vibration, and C–O in-plane deformation vibration, respectively. The presence of these characteristic peaks confirms the existence of $CaCO_3$ in the waterborne primers. Moreover, the appearance of the characteristic peak at 1392 cm^{-1} in the composite primer spectra indicates the presence of hydroxyl functional groups; the higher the hydroxyl content, the stronger the hydroxylation performance. Under the influence of the waterborne solution, TiO_2 can encapsulate $CaCO_3$ to form stable precipitation, leading to improved film performance of the cured coating [36]. These observations indicate the successful application of a new primer coating material, TiO_2@$CaCO_3$, on the wood surface.

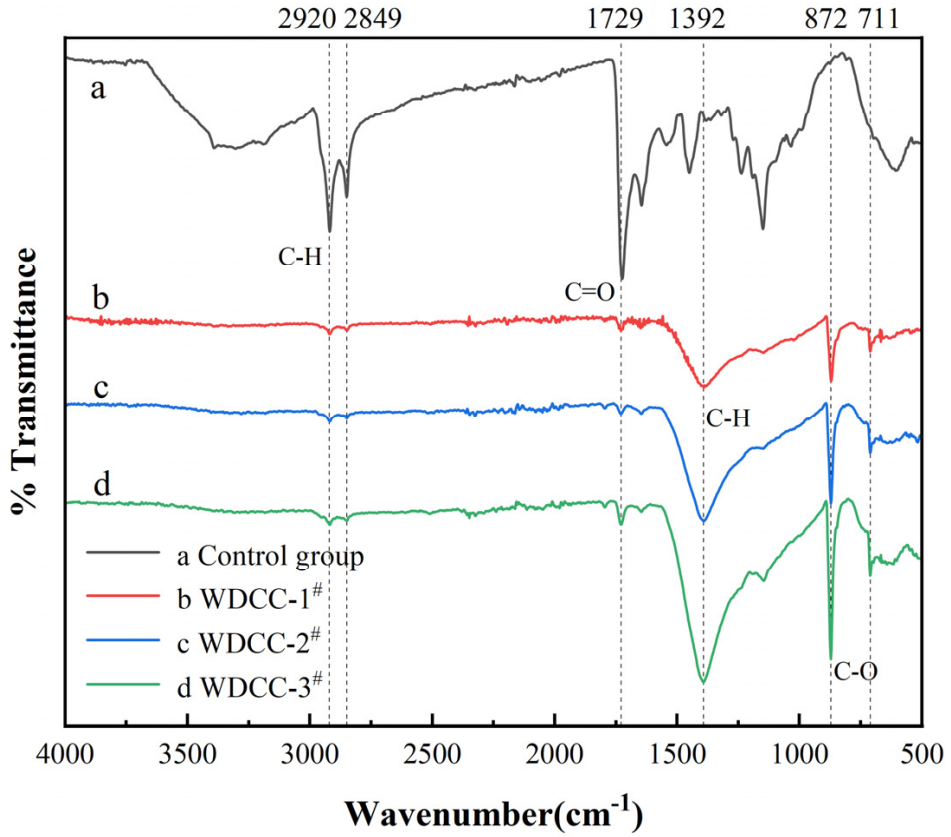


Figure 4. Infrared spectra of wood coated with composite water-based primers with different TiO_2-to-$CaCO_3$ ratios.

3.3. Surface Morphology Characteristics of TiO_2@$CaCO_3$ Water-Based Primer Coatings

Figure 5 presents scanning electron microscopy images of the three composite water-based primer coatings with different TiO_2-to-$CaCO_3$ mass ratios. The WDCC-1# coating, with a ratio of 5:45, exhibits significant agglomeration, resulting in an uneven surface (Figure 5A). This effect is attributable to the excessive calcium carbonate content in WDCC-1#, which adversely affects the subsequent inkjet printing of the dye coating due to reduced resolution. The WDCC-2# coating, with a ratio of 10:40, features less pronounced aggregation in microstructure than WDCC-1# (Figure 5B). The WDCC-3# coating, with a ratio of 15:35, features the most uniform microstructure, characterized by a dense and uniform particle structure (Figure 5C). The comparison of the microstructures of the three coatings with different filler ratios reveals that as the $CaCO_3$ content increases, the coating agglomeration becomes more severe. This highlights the influence of the $CaCO_3$ content on coating smoothness, emphasizing the need for coordination between the $CaCO_3$ and TiO_2 contents. Excessive differences in the mass fraction of these two components can lead to uneven chemical reactions, resulting in the accumulation and agglomeration of $CaCO_3$. To further investigate the permeability of the composite water-based primer coating, the elemental distributions of TiO_2 and $CaCO_3$ in the sample section were analyzed using an energy-dispersive spectrometer mode. The colored dot area in Figure 5D–F shows that Ti and Ca elements are densely concentrated on the wood surface.

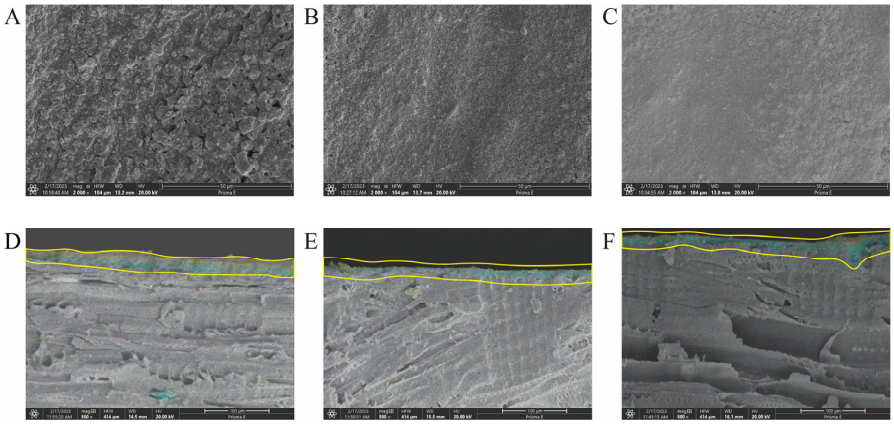


Figure 5. Scanning electron microscopy (SEM) and energy-dispersive X-ray spectroscopy (EDS) images of waterborne primer coatings with different filler ratios. (**A**) SEM image of the surface of oak multilayer boards coated with WDCC-1#; (**B**) SEM image of the surface of oak multilayer boards coated with WDCC-2#; (**C**) SEM image of the surface of oak multilayer boards coated with WDCC-3#; (**D**) The yellow area of the EDS spectra show the presence of Ti and Ca elements on the surface of oak boards coated with WDCC-1#; (**E**) The yellow area of the EDS spectra show the presence of Ti and Ca elements on the surface of oak boards coated with WDCC-2#; (**F**) The yellow area of the EDS spectra show the presence of Ti and Ca elements on the surface of oak boards coated with WDCC-3#.

3.4. Microscopic Observation of Ink Dot Morphology Characteristics of Inkjet Printing Coatings

Electron microscopy images of TiO_2@$CaCO_3$ composite aqueous primer coatings and aqueous inkjet print patterns are displayed in Figure 6. Figure 6A–C presents microscopic images of the waterborne primer coatings with three filler ratios at a 10× magnification. The roller-coated surface shown in Figure 6a appears relatively rough, making it challenging to effectively cover the wood grain crevices. Figure 6b also shows primer build-up with noticeable granularity and unevenness, whereas Figure 6c presents a relatively finer coating. These features indicate that the quantity of calcium carbonate added to the mixture influences the dispersion quality of the coating. An excess of calcium carbonate, exceeding 40% of the total component, presumably leads to particle aggregation into clusters. Additionally, oak boards possess a rough, mountainous surface with long rays that contribute to the wood's natural texture but also affect the evenness of paint adhesion. The morphology of ink droplets spreading on the substrate directly affects the print quality of inkjet patterns. The formation of droplet states is influenced by the substrate surface quality and the settings of the printing process parameters. Further research into process parameter optimization will require new experimental explorations.

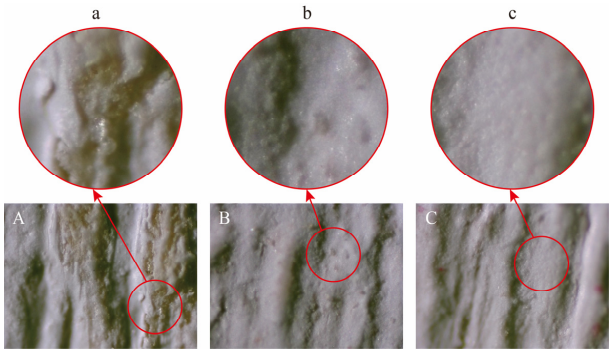


Figure 6. (**A–C**) Electron microscopy images of TiO_2@$CaCO_3$ composite waterborne primer coatings (10×, (**a**) Magnified view of WDCC-1# primer coating details; (**b**) Magnified view of WDCC-2# primer coating details; (**c**) Magnified view of WDCC-3# primer coating details).

3.5. Analysis of the Coloring Performances of TiO_2@$CaCO_3$ Waterborne Primers

The effect of the TiO_2@$CaCO_3$ composite aqueous primer on the coloring effect of aqueous inkjet printing patterns is presented in Figure 7. Figure 7A presents a standard CMYK digital image. The color difference values between Figure 7C–E and Figure 7A are detailed in Table 4. The line graph in Figure 7F illustrates that WDCC-3# produces a printed ink image with minimal color deviation and superior color reproduction. Figure 7B reveals that the color of inkjet prints on the surface of a substrate lacking a primer coating significantly deviates from the standard color. This discrepancy arises from the wood's inherent hydrophilicity, as the pigments (e.g., tannic acid) contained in wood are also hydrophilic, and water constitutes a major component of water-based ink coatings. When ink is applied to the wood surface, the colored components within the wood rapidly dissolve into the continuous phase of the coating water, similar to adding color to the coating. This alteration affects the color phase of the coating [16]. Hence, the introduced primer coating functions as a transitional layer that connects the ink layer and the substrate. The coating ensures that the sprayed ink does not blend with the colored components in the wood, preventing discoloration and maximizing color saturation.

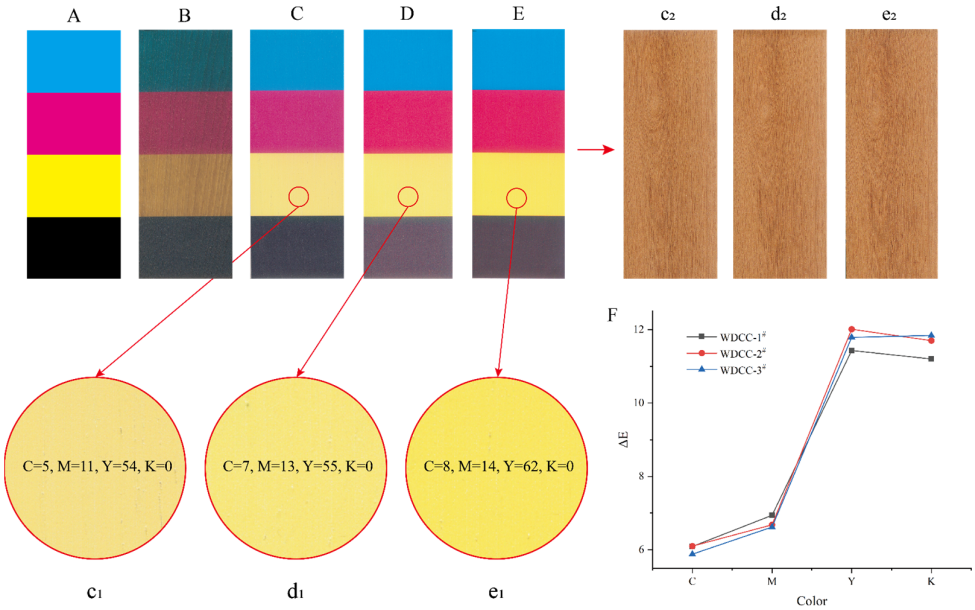


Figure 7. (**A**) Photoshop production of CMYK color block image; (**B**) Inkjet-printed CMYK image without primer treatment; (**C**–**E**) Inkjet-printed CMYK color block image of waterborne primer with different filler ratios (**C** WDCC-1#, **D** WDCC-2#, **E** WDCC-3#); (**c_1**–**e_1**) Magnified color difference of yellow waterborne ink in CMYK color block for inkjet printing; (**c_2**–**e_2**) Effect of inkjet-printed wood grain pattern of TiO_2@$CaCO_3$ composite waterborne primer with different filler ratios; (**F**) Color differences in the inkjet printing of CMYK color blocks, represented as a folded line graph.

The introduction of the TiO_2@$CaCO_3$ water-based primer coating significantly reduces the color shift of the topcoat coating. However, the adhesion of the primer to the substrate is not as strong as that of the WD4500A water-based polyurethane resin primer because water-based polyurethane resin has excellent permeability and can penetrate the substrate's capillaries, thereby preventing the leakage of pigments or tannic acid [30]. When used as the initial layer in the roller-coating process, the water-based polyurethane resin primer can fully demonstrate its advantages. However, it exhibits weak ink absorption ("fixed ink"), resulting in a less satisfactory color rendering effect for inkjet-dyed wood product coatings. Hence, combining the composite primer with the water-based polyurethane resin primer can better leverage the advantages of both primers.

Table 4. Standard values of color samples, actual values of test samples, and color difference values.

Color Sample		C	M	Y	K
Standard value	L^*	58	49	94	10
	a^*	−41	82	−8	5
	b^*	−54	−4	105	4
WDCC-1#	L^*	52.54	43.32	88.12	23.06
	a^*	−32.11	63.95	−8.36	9.99
	b^*	−46.50	−1.98	56.34	−1.65
	ΔE_{00}	6.09	6.94	11.43	11.2
WDCC-2#	L^*	52.46	43.63	87.61	23.44
	a^*	−32.58	64.23	−6.08	10.25
	b^*	−46.24	−1.76	53.53	−2.23
	ΔE_{00}	6.1	6.68	12.01	11.7
WDCC-3#	L^*	52.74	43.77	87.56	23.28
	a^*	−32.45	64.02	−6.18	10.44
	b^*	−46.33	−1.63	54.45	−2.70
	ΔE_{00}	5.88	6.62	11.79	11.84

Figure 7(c_2–e_2) shows the primer treatment and inkjet printing on the oak plank plate. The water-based primer with $CaCO_3$ presents a more delicate spray printing pattern, with little difference in resolution compared with the original digitally scanned wood grain image. After coating with the composite primer, the oak plank is inkjet-printed, resulting in a firmer texture of wood grain pattern printing. Most of the mountain grain unevenness of the wood is covered and smoothed by the primer so that the wood's natural texture is lost. This coating method is more suitable for wood with surface scars and stains and can improve the decorative appeal of such wood.

3.6. Determination of Paint Film Performance

The application of $CaCO_3$ as a functional filler can significantly reduce the production cost of coatings and enhance various paint film properties [18]. In addition to serving as a system pigment, $CaCO_3$ can undergo hydrolysis to form calcium hydroxide, which in turn improves substrate adhesion, absorbs acidic media, and contributes to rust prevention. With the addition of $CaCO_3$ filler, the coating film exhibits a semi-smooth rough surface, which promotes adhesion to the upper coating and enhances the coating film's adhesion [14,16]. Table 5 demonstrates that the adhesion of the TiO_2@$CaCO_3$ composite water-based primer is excellent, achieving a level 1 rating in compliance with national coating standards. However, the excessive or insufficient use of $CaCO_3$ does not yield the desired effect in improving paint film performance. The incorporation of fillers tends to result in an overall reduction in the glossiness of the paint film. The application of excessive quantity significantly reduces the paint film's glossiness, while hardness and roughness increase. Compared with the other primers, WDCC-3# exhibits superior surface smoothness and whiteness.

Table 5. Determination of TiO_2@$CaCO_3$ waterborne primer film.

Grouping	Adhesion	Glossiness	Durometer	Roughness	Whiteness
WDCC-1#	Level 1	5.12	6H	3.225	66.12
WDCC-2#	Level 1	5.68	4H	2.518	68.34
WDCC-3#	Level 1	5.8	4H	2.33	70.52

4. Conclusions

The effect of a composite water-based primer with TiO_2 and $CaCO_3$ fillers on the coloring performance of water-based inkjet coatings was studied. The WDCC-3# water-based primer exhibited the most comprehensive performance.

(1) At a TiO_2-to-$CaCO_3$ ratio of approximately 15:35, the prepared primer coating effectively improved the compatibility between water-based ink and the wooden substrate. The contact angle of water-based ink droplets was only 5.8°, indicating superior ink fixation performance. The water-based inkjet coating could rapidly penetrate the primer layer.
(2) The combination of $CaCO_3$ and TiO_2 led to robust hydroxylation performance. Under the influence of the waterborne solution, TiO_2 could encapsulate $CaCO_3$ to form stable precipitation. This enhanced the waterproofing and permeability of the paint film.
(3) The surface of the WDCC-3# primer coating was exceptionally smooth, with minimal agglomeration. Digital inkjet-printed water-based ink droplets appeared more uniform and transparent, with rare occurrences of the "coffee rings". This advantage translates to higher resolution and finer image quality for the sprayed wood grain.
(4) In terms of paint film characteristics, compared with the other primers, WDCC-3# exhibited better glossiness, higher whiteness, and minor roughness, resulting in more pronounced and stable printing effects.

Overall, in addition to concealing knots and stains on the substrate's surface, the waterborne primer layer also plays a crucial role as a coating bridge connecting the topcoat and the wooden substrate. This study not only explores enhanced water-based primers from the perspective of component modification but also elucidates how the water-based wood product coating process influences the performance of water-based inkjet coatings. Each water-based primer has its own set of advantages and disadvantages. Achieving the best-performing coating involves applying water-based primers with various strengths in different coating processes. This approach opens up new possibilities for utilizing water-based primers in water-based wood product coating processes. Moreover, the approach paves the way for realizing the "digital production of wood products" through intelligent manufacturing, rapidly enhancing the decorative and economic value of wood products.

Author Contributions: Conceptualization, methodology, validation, resources, data management, supervision, review, R.S.; formal analysis, investigation, writing (original draft), F.Y. All authors have read and agreed to the published version of the manuscript.

Funding: This research was funded by the Natural Science Foundation of Jiangsu Province (BK20190750) and the Youth Science and Technology Innovation Fund of Nanjing Forestry University (CX2019017).

Institutional Review Board Statement: Not applicable.

Informed Consent Statement: Not applicable.

Data Availability Statement: Data is contained within the article.

Conflicts of Interest: The authors declare no competing financial interest.

References

1. Zhao, L.; Hong, C.; Wang, C.; Li, J.; Ren, H.; Zhou, C. Enhancement of the adhesion strength of water-based ink binder based on waterborne polyurethane. *Prog. Org. Coat.* **2023**, *183*, 107765. [CrossRef]
2. Jingxiang, X.; Jinyao, L.; Haichao, L.; Mingming, Z.; Jifei, C. Research Progress on Water-based Ink Drying Technology. *IOP Conf. Ser. Mater. Sci. Eng.* **2019**, *565*, 012017. [CrossRef]
3. Sang, R.; Manley, A.J.; Wu, Z.; Feng, X. Digital 3D Wood Texture: UV-Curable Inkjet Printing on Board Surface. *Coatings* **2020**, *10*, 1144. [CrossRef]
4. Zhu, J.; Wu, Z.; Xiong, D.; Pan, L.; Liu, Y. Preparation and properties of a novel low crystallinity cross-linked network waterborne polyurethane for water-based ink. *Prog. Org. Coat.* **2019**, *133*, 161–168. [CrossRef]
5. Xiong, X.; Niu, Y.; Yuan, Y.; Zhang, L. Study on Dimensional Stability of Veneer Rice Straw Particleboard. *Coatings* **2020**, *10*, 558. [CrossRef]
6. Peng, W.X.; Zhang, X.; Deng, H.P.; Li, K.F.; Fan, Z.C.; Peng, W.L. Study on Ecological Management Mode of Finishing Technology of Wood Multi-layer Floor in China. In Proceedings of the 2009 International Conference on Electronic Commerce and Business Intelligence, Beijing, China, 6–7 June 2009; Volume 294.
7. Chen, Y.; Sun, C.; Ren, Z.; Na, B. Review of the current state of application of wood defect recognition technology. *BioResources* **2022**, *18*, 49. [CrossRef]

8. Ozcan, A.; Sonmez, S.; Tutak, D. Effect of coating pigment type on paper printability with water-based inks. *J. Coat. Technol. Res.* **2022**, *19*, 1149–1157. [CrossRef]
9. Javadi, A.; Cobaj, A.; Soucek, M.D. *Handbook of Waterborne Coatings*; Elsevier: Amsterdam, The Netherlands, 2020; pp. 303–344.
10. Yan, X.; Peng, W. Preparation of Microcapsules of Urea Formaldehyde Resin Coated Waterborne Coatings and Their Effect on Properties of Wood Crackle Coating. *Coatings* **2020**, *10*, 764. [CrossRef]
11. Soula, M.; Profili, J.; Caceres-Ferreira, W.; Samyn, F.; Duquesne, S.; Falzacappa, E.V.; Scopece, P.; Laroche, G.; Landry, V. Effect of a thin organosilicon layer prepared by atmospheric pressure plasma on wood flame retardancy. *Plasma Process. Polym.* **2022**, *19*, 2200051. [CrossRef]
12. Böger, T.; Sanchez-Ferrer, A.; Richter, K. Hydroxymethylated resorcinol (HMR) primer to improve the performance of wood-adhesive bonds—A review. *Int. J. Adhes. Adhes.* **2022**, *113*, 103070. [CrossRef]
13. Peng, X.; Zhang, Z. Improvement of paint adhesion of environmentally friendly paint film on wood surface by plasma treatment. *Prog. Org. Coat.* **2019**, *134*, 255–263. [CrossRef]
14. Krapež Tomec, D.; Balzano, A.; Žigon, J.; Šernek, M.; Kariž, M. The Effect of Printing Parameters and Wood Surface Preparation on the Adhesion of Directly 3D-Printed PLA on Wood. *J. Renew. Mater.* **2022**, *10*, 1787–1796. [CrossRef]
15. Hermann, A.; Giljean, S.; Pac, M.-J.; Marsiquet, C.; Burr, D.; Landry, V. Physico-mechanical characterisation of basecoats for tailored UV-cured multilayered wood coating systems. *Prog. Org. Coat.* **2023**, *182*, 107673. [CrossRef]
16. Hermann, A.; Giljean, S.; Pac, M.-J.; Marsiquet, C.; Beaufils-Marquet, M.; Burr, D.; Landry, V. Understanding indentation, scratch and wear behavior of UV-cured wood finishing products. *Prog. Org. Coat.* **2021**, *161*, 106504. [CrossRef]
17. Liu, W.; Hu, C.; Zhang, W.; Liu, Z.; Shu, J.; Gu, J. Modification of birch wood surface with silane coupling agents for adhesion improvement of UV-curable ink. *Prog. Org. Coat.* **2020**, *148*, 105833. [CrossRef]
18. Scotton, R.S.; Guerrini, L.M.; Oliveira, M.P. Evaluation of solvent-based and UV-curing inkjet inks on the adhesion and printing quality of different aircraft surfaces coating. *Prog. Org. Coat.* **2021**, *158*, 106389. [CrossRef]
19. Sang, R.; Yang, F.; Fan, Z. The Effect of Water-Based Primer Pretreatment on the Performance of Water-Based Inkjet Coatings on Wood Surfaces. *Coatings* **2023**, *13*, 1649. [CrossRef]
20. Yan, X.; Li, W.; Han, Y.; Yin, T. Preparation of Melamine/Rice Husk Powder Coated Shellac Microcapsules and Effect of Different Rice Husk Powder Content in Wall Material on Properties of Wood Waterborne Primer. *Polymers* **2021**, *14*, 72. [CrossRef]
21. Yan, X.; Pan, P. Preparation of Silver Antibacterial Agents with Different Forms and Their Effects on the Properties of Water-Based Primer on Tilia europaea Surface. *Coatings* **2021**, *11*, 1066. [CrossRef]
22. Li, Z.; Huang, C.; Guo, L.; Cui, L.; Zhou, B. Mass production and application of TiO_2@$CaCO_3$ composites in interior emulsion coatings. *Colloids Surf. A Physicochem. Eng. Asp.* **2016**, *498*, 98–105. [CrossRef]
23. Tao, H.; He, Y.; Zhao, X. Preparation and characterization of calcium carbonate–titanium dioxide core–shell ($CaCO_3$@TiO_2) nanoparticles and application in the papermaking industry. *Powder Technol.* **2015**, *283*, 308–314. [CrossRef]
24. Sun, S.; Ding, H.; Zha, Y.; Chen, W.; Xu, Z. Surface Organic Modification of CaCO3-TiO2 Composite Pigment. *Minerals* **2019**, *9*, 112. [CrossRef]
25. Yang, H.; Mu, B.; Li, S.; Wang, N.; Hui, A.; Wang, A. $CaCO_3$-assisted mechanochemical synthesis of low-cost and high-chroma cobalt blue composite pigments using kaolin tailing sand for ceramic coloring. *J. Ind. Eng. Chem.* **2022**, *112*, 440–450. [CrossRef]
26. *ISO 11664-6:2022*; Colorimetry—Part 6: CIEDE2000 Colour-Difference Formula. ISO: Geneva, Switzerland, 2022.
27. *GB/T 4893.4-2013*; Test for Physical and Chemical Properties of Paint Film on Furniture Surfaces—Part 4: Determination of Adhesion by Cross Cutting. Standards Press of China: Beijing, China, 2013.
28. *GB/T 4893.6-2013*; Test for Physical and Chemical Properties of Paint Film on Furniture Surfaces—Part 6: Glossometry. Standards Press of China: Beijing, China, 2013.
29. *GB/T 6739-2006*; Determination of Paint Film Hardness by Pencil Method for Paint and Varnish. Standards Press of China: Beijing, China, 2006.
30. Sang, R.; Yang, S.; Fan, Z. Effects of MDF Substrate Surface Coating Process on UV Inkjet Print Quality. *Coatings* **2023**, *13*, 970. [CrossRef]
31. Chen, J.; Zhang, K.; Zhang, K.; Yang, L.; Jiang, B. The research progress in recording layer of the inkjet printing materials. *J. Appl. Polym. Sci.* **2021**, *138*, 50894. [CrossRef]
32. Zhang, M.; Lyu, J.; Zuo, Y.; Li, X.; Li, P. Effect of KH560 concentration on adhesion between silicate modified poplar and waterborne varnish. *Prog. Org. Coat.* **2023**, *174*, 107267. [CrossRef]
33. Wang, T.; Jia, S.; Xu, Y.; Dong, Y.; Guo, Y.; Huang, Z.; Li, G.; Lian, J. Improving the corrosion resistance and biocompatibility of magnesium alloy via composite coatings of calcium phosphate/carbonate induced by silane. *Prog. Org. Coat.* **2022**, *163*, 106653. [CrossRef]
34. Hao, W.; Zheng, Q.; Zhong, Y.; Meng, X.; Wang, H.; Qiu, L.; Lu, H.; Huang, Y.; Yang, W. An eco-friendly and facile method to prepare waterborne polyurethane based fire-resistant & waterproof coatings for wood protection. *Prog. Org. Coat.* **2023**, *185*, 107892.

35. Chen, T.; Xu, G.; Bao, J.; Huang, Y.; Yang, W.; Hao, W. One-pot preparation of hydrogel wound dressings from Bletilla Striata polysaccharide and polyurethane with dual network structure. *Eur. Polym. J.* **2022**, *181*, 111648. [CrossRef]
36. Chen, G.; Liu, Y.; Fang, Z. Preparation of titanium dioxide-calcium carbonate composite filler and its application in paper making. *J. South China Univ. Technol. Nat. Sci. Ed.* **2011**, *39*, 87–92.

Disclaimer/Publisher's Note: The statements, opinions and data contained in all publications are solely those of the individual author(s) and contributor(s) and not of MDPI and/or the editor(s). MDPI and/or the editor(s) disclaim responsibility for any injury to people or property resulting from any ideas, methods, instructions or products referred to in the content.